

## Short communication

## Influence of the support in aqueous phase oxidation of ethanol on gold/metal oxide catalysts studied by ATR-IR spectroscopy under working conditions

Ammara Waheed<sup>a,b</sup>, Xianwei Wang<sup>c</sup>, Nobutaka Maeda<sup>d,\*</sup>, Daniel.M. Meier<sup>d</sup>, Tamao Ishida<sup>e,\*</sup>, Toru Murayama<sup>e</sup>, Masatake Haruta<sup>e</sup>, Alfons Baiker<sup>f,\*</sup><sup>a</sup> Gold Catalysis Research Center, State Key Laboratory of Catalysis, Dalian Institute of Chemical Physics, Chinese Academy of Sciences, 457 Zhongshan Road, Dalian 116023, People's Republic of China<sup>b</sup> University of Chinese Academy of Sciences, Beijing 100049, China<sup>c</sup> Key Laboratory of Industrial Ecology and Environmental Engineering, School of Environmental Science and Technology, Dalian University of Technology, Dalian 116024, People's Republic of China<sup>d</sup> Institute of Materials and Process Engineering (IMPE), Zurich University of Applied Sciences (ZHAW), Technikumstrasse 9, CH-8400 Winterthur, Switzerland<sup>e</sup> Department of Applied Chemistry for Environment, Research Center for Gold Chemistry, Graduate School of Urban Environmental Sciences, Tokyo Metropolitan University, 1-1 Minami-Osawa, Hachioji, Tokyo 192-0397, Japan<sup>f</sup> Institute for Chemical and Bioengineering, Department of Chemistry and Applied Biosciences, ETH Zurich, Hönggerberg, HCI, CH-8093 Zurich, Switzerland

## ARTICLE INFO

## Keywords:

Ethanol oxidation

Acetic acid

Gold catalysis

Effect of support

In situ ATR-IR spectroscopy

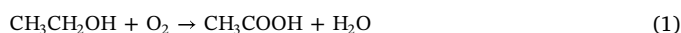
## ABSTRACT

Effects of supports (Co<sub>3</sub>O<sub>4</sub>, CeO<sub>2</sub>, NiO) in the gold-catalyzed aqueous phase oxidation of ethanol (EtOH) to acetic acid (AcOH) were examined. ATR-IR spectroscopy under working conditions of the catalysts uncovered on gold particles bidentate ethoxy, and on supports monodentate ethoxy species, multi-layered ethanol, and acetate. Preferential formation of bidentate ethoxy species and adsorbed EtOH were identified as key factors for high activity and selectivity to AcOH. These requirements were best matched with Au/Co<sub>3</sub>O<sub>4</sub>. On NiO, monodentate ethoxy species on the support deteriorated the catalytic performance due to consecutive esterification of AcOH and/or acetate species with EtOH producing undesirable ethyl acetate.

## 1. Introduction

Bio-ethanol is one of the promising products of the chemical conversion of biomass, which is a sustainable chemical feedstock to synthesize chemicals more simply and in fewer industrial steps [1]. The biomass-derived ethanol can be further employed to produce isobutene [2], 2-propanone [3], *n*-butanol [4], ethyl acetate [5], 1,3-butadiene [6], propene [7], and acetic acid [8]. One of the most desirable products in the ethanol conversion is acetic acid, which is used as a raw material for the production of various chemicals, such as acetic anhydride, vinyl acetate monomer, terephthalic acid, and various acetates [9]. Conventional industrial inorganic oxidants, e.g. permanganate and dichromate, are poisonous and leave a large amount of waste. From both environmental and economic point of view, there is an emergent need to develop a green process by employing clean oxidants [10], such as O<sub>2</sub>, and more efficient and reusable heterogeneous catalysts instead of acids for the production of acetic acid [11]. Heterogeneous catalysis requires relatively mild reaction conditions, low pressure and low

temperature with molecular oxygen as an oxidant [12] according to:



Noble metal nanoparticles supported on metal oxides are known to catalyze the ethanol oxidation with molecular oxygen in water [13]. Specifically, Pd- and Pt-based catalysts outperform any other catalysts [14]. Even a small content of Pd (0.5 wt%) was found to be efficient for the selective oxidation of ethanol to acetic acid. In particular, the use of alumina as support produced by combustion synthesis contributes to high ethanol conversion (> 90%) and selectivity (> 60%) to acetic acid [15]. The nature of the support material drastically influences the product distribution. Pt/Al<sub>2</sub>O<sub>3</sub> produces acetic acid as the main product while Pt/ZrO<sub>2</sub>, Pt/CeO<sub>2</sub>, and Pt/Ce<sub>0.50</sub>Zr<sub>0.50</sub>O<sub>2</sub> produce methane and acetaldehyde [16]. However, what is common to Pt and Pd-based catalysts, is the low selectivity to acetic acid at high ethanol conversions [9].

Gold catalysts were also reported to catalyze the oxidation of higher alcohols to corresponding carboxylic acids [17]. Compared to Pt-based

\* Corresponding authors.

E-mail addresses: [maeo@zhaw.ch](mailto:maeo@zhaw.ch) (N. Maeda), [tamao@tmu.ac.jp](mailto:tamao@tmu.ac.jp) (T. Ishida), [alfons.baiker@chem.ethz.ch](mailto:alfons.baiker@chem.ethz.ch) (A. Baiker).<https://doi.org/10.1016/j.catcom.2020.106183>

Received 27 July 2020; Received in revised form 4 September 2020; Accepted 4 October 2020

Available online 06 October 2020

1566-7367/© 2020 Elsevier B.V. This is an open access article under the CC BY-NC-ND license (<http://creativecommons.org/licenses/by-nc-nd/4.0/>).

catalysts, Au catalysts offer high conversion and selectivity for the liquid-phase oxidation of various alcohols [18]. Au/MgAl<sub>2</sub>O<sub>4</sub>, Au/ZnO, Au/Al<sub>2</sub>O<sub>3</sub>, and Au/TiO<sub>2</sub> catalysts were reported to afford high conversion and selectivity [11,19]. Especially, Au/ZnO used with a slight excess of molecular oxygen showed an excellent catalytic performance (99.4% ethanol conversion at 99.8% selectivity to acetic acid) [11]. Compared to the gas-phase oxidation of ethanol over vanadia-based catalysts [20], which also shows a significant influence of the support, the liquid-phase oxidation on Au-based catalysts can be operated at lower temperature and affords high conversion and selectivity to acetic acid. The selectivity to acetic acid or ethyl acetate is significantly influenced by the choice of the support material; CeO<sub>2</sub>, Al<sub>2</sub>O<sub>3</sub>, and NiO as supports mainly form acetic acid, whereas BaO and Co<sub>3</sub>O<sub>4</sub> offer high selectivity to ethyl acetate [9]. Takei et al. screened twelve kinds of single metal oxides supports for Au nanoparticles, among them NiO showed the highest conversion of ethanol and good selectivity to acetic acid [9]. However, the trend of the catalytic activity differs depending on the preparation method of the catalysts, i.e., co-precipitation, deposition-precipitation, and solid grinding methods [9].

There has been significant progress in developing Au catalysts based on different support materials but the underlying mechanisms and selectivity-controlling factors induced by the different type of supports remains unclear. In this work, we applied in situ attenuated total reflectance Fourier transform infrared (ATR-IR) spectroscopy to gain a deeper understanding of the role of the key intermediates, surface species, and reaction mechanism. To the best of our knowledge, this is the first report on IR analysis of the surface processes in the aqueous phase oxidation of ethanol under working conditions (higher pressure and temperature) and it highlights the role of ethoxy species as a selectivity-controlling factor.

## 2. Experimental

### 2.1. Materials

To investigate the support effects in the gold-catalyzed aqueous phase oxidation of ethanol to acetic acid, we employed standard Au catalysts provided by Haruta Gold Inc. (HGI) in Japan because the properties of these catalysts are well-defined with minimum deviation. The characterization data provided by HGI is shown in Table 1.

### 2.2. IR spectroscopy

For in situ ATR-IR spectroscopic analysis of the catalytic solid-liquid interfaces at higher temperature and pressure, thin films of the catalyst powder were prepared as follows. 180 mg of fine catalyst powders were suspended in 24 mL of ethanol and the resulting slurry was ultrasonicated for 30 min to obtain a uniform suspension. 2.0 mL of the slurry (corresponding to a catalyst loading of  $15 \pm 1$  mg) was slowly placed drop by drop using a pipet over a square internal reflection element (IRE, with a bevel of 45°, 1 mm × 1 mm) located in IR cell (Golden Gate™ ATR, SPECAC) and the ethanol was evaporated overnight at room temperature. This procedure guarantees that the catalyst layer adhered to the IRE crystal such that no loss of the catalyst occurs [21,22]. A diamond IRE was selected to avoid full absorption of mid-IR light by water because of its relatively low penetration depth of the

evanescent wave. The diamond IRE also enables in situ measurement under severe conditions [21–24]. IR spectra were recorded on a Vertex 70v spectrometer (Bruker) equipped with a liquid nitrogen-cooled mercury-cadmium-telluride (MCT) detector (ID316, ZnSe Window) and an optical filter (F321). The spectra were taken at 4 cm<sup>-1</sup> of the spectral resolution and 60 kHz of the scanning velocity. 64 scans (in total < 5 s) were co-added for each spectrum. Before the spectral acquisition, the beamline compartment of the spectrometer was vacuumed to < 1 kPa to enhance the brightness of the IR beam. A water-cooled globar Mid-IR source with high output power was applied to enhance the amplitude and the signal-to-noise (S/N) ratio.

### 2.3. Catalytic performance test and IR measurements

5 mL of a reaction mixture (5, 20, and 40 vol% ethanol in water) was added to the reactor taking care that the catalyst layer was not detached from the diamond IRE. Then, the reactor was purged with helium (100 mL/min) for 5 min to replace the air, followed by O<sub>2</sub>-purge for 5 min and pressurization to 3 bar. The reactor was then quickly heated to 120 °C within 5 min. As soon as the temperature reached 120 °C, a spectral background was taken, followed by repeated spectral measurements for 2 h at an interval of 5 min (24 spectra). Therefore, the initially measured background was subtracted from all the subsequent spectra acquired. Each experiment under the same condition was repeated three times for reproducibility. This procedure guarantees in situ monitoring of active surface species, which change over the time course and removal of surface and bulk (EtOH and H<sub>2</sub>O in the liquid phase) species not involved in the reaction [22]. The compositions in the liquid phase were analyzed with a gas chromatograph equipped with a flame ionization detector (FID-GC). After the reaction, 60 mg of 1,2-dimethoxyethane was added to the reaction mixture as an internal standard, followed by filtration and dilution with 1,4-dioxane. Acetaldehyde (AcH), ethyl acetate (AcOEt), and acetaldehyde diethyl acetal (Acetal) were analyzed with an FID-GC (Agilent GC7890A) equipped with a capillary (5%-phenyl)-methylpolysiloxane nonpolar column (J&W HP-5). Ethanol (EtOH) and acetic acid (AcOH) were analyzed with an FID-GC (SHIMADZU Tracer) equipped with a capillary polyethylene glycol column (VF-WAXms).

## 3. Results and discussion

The catalytic performance of the catalysts consisting of gold nanoparticles supported on different metal oxide supports in the aqueous phase oxidation of ethanol at 120 °C and 3 bar are summarized in Table 2. Clearly, the catalytic performance of the Au catalysts was significantly influenced by the nature of the support. Among the three different support materials, Au/Co<sub>3</sub>O<sub>4</sub> showed the highest conversion (46.6%) and selectivity to AcOH (79.3%). The EtOH conversion on the catalysts followed the order Co<sub>3</sub>O<sub>4</sub> > NiO > CeO<sub>2</sub>, while the selectivity to AcOH obeyed the trend: Co<sub>3</sub>O<sub>4</sub> > CeO<sub>2</sub> > NiO. The low carbon balance for Au/NiO resulted from the formation of CO<sub>2</sub> via unfavorable overoxidation [9]. In the given ranges neither the Au particle size nor the BET surface area were markedly relevant for the catalytic performance achieved with these catalysts, as the corresponding data listed in Tables 1 and 2 indicate. However, the nature of the support material and possibly its perimeter with the deposited Au

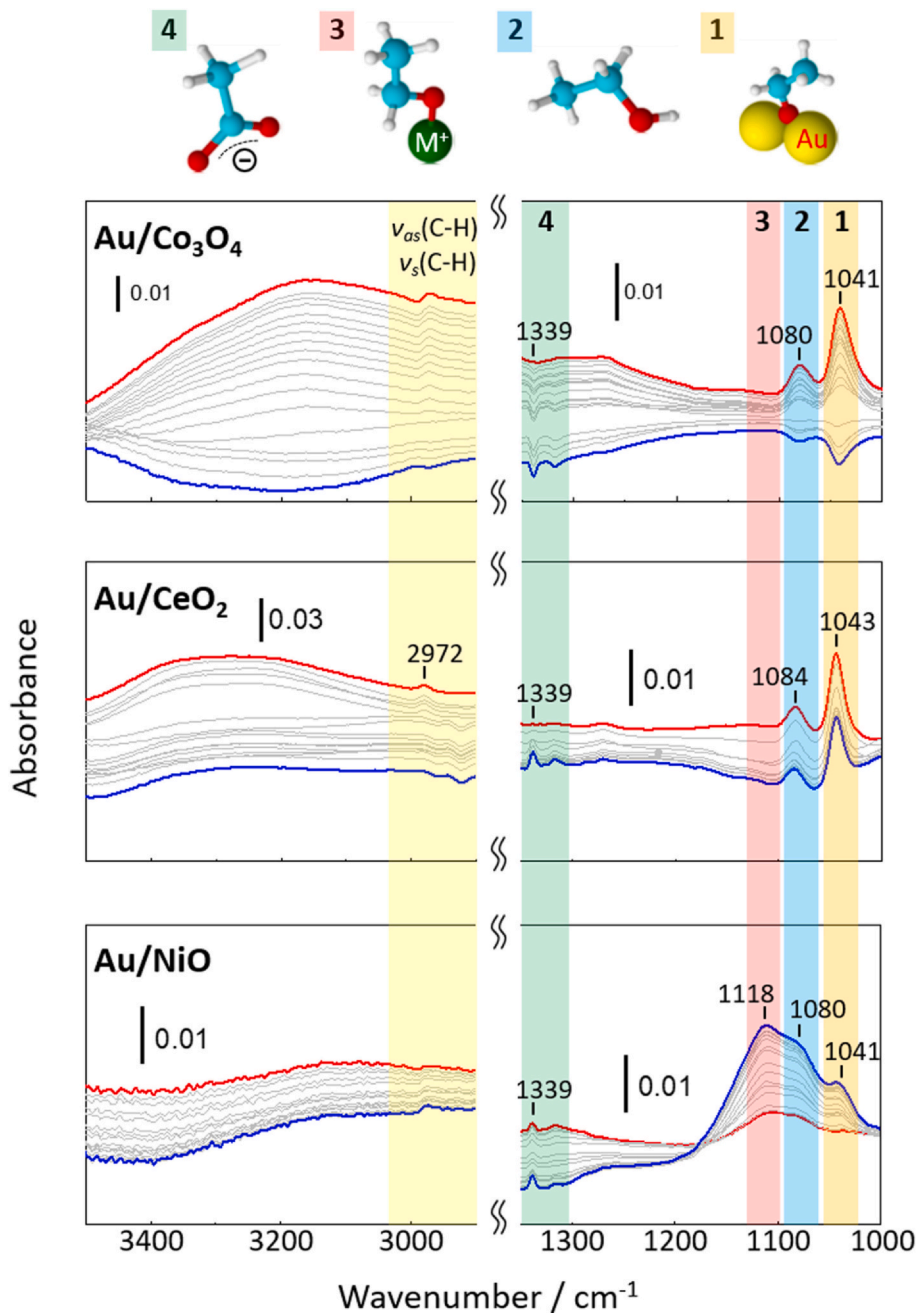
**Table 1**  
Characterization data of Au catalysts provided by HGI.

Catalyst	Au loading (wt%)	Au particle size (nm)	BET surface area (m <sup>2</sup> /g)	Mean diameter of support particles (μm)
Au/NiO	0.93	— <sup>a</sup>	256	5.9
Au/CeO <sub>2</sub>	0.98	4.5	20	5.1
Au/Co <sub>3</sub> O <sub>4</sub>	1.00	1.8	102	2.0

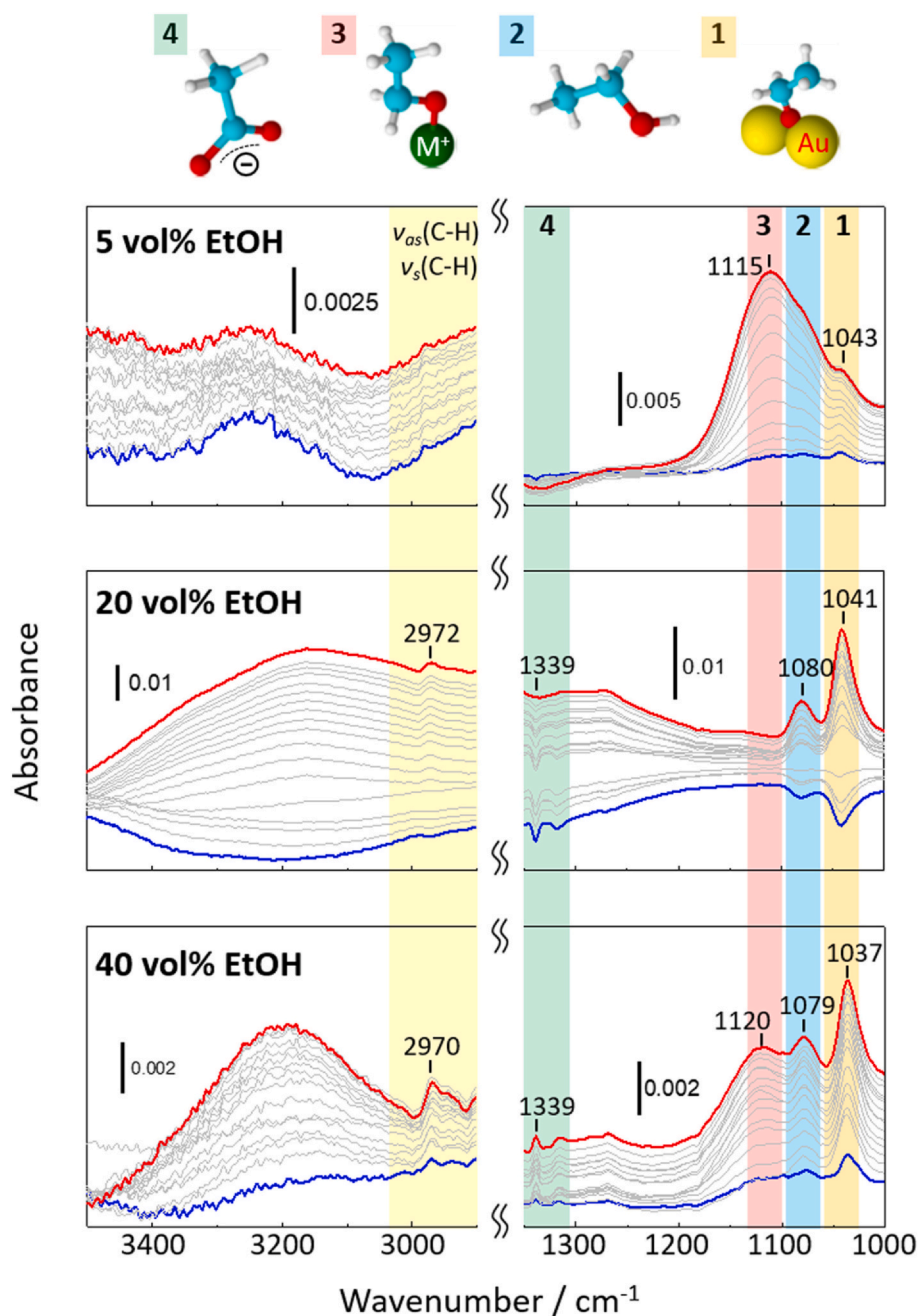
<sup>a</sup> Au particles were not observable by transmission electron microscopy because of the poor contrast between Au and NiO.

Table 2

Catalyst	EtOH (Vol%)	Conversion (%)	AcH <sup>a</sup> (%)	AcOEt <sup>a</sup> (%)	Acetal <sup>a</sup> (%)	AcOH <sup>b</sup> (%)	Selectivity to AcOH (%)	Total yield (%)	Carbon balance (%)
Au/CeO <sub>2</sub>	20	11.8	3.3	3.1	0.0	3.9	33.0	10.3	87.4
Au/NiO	20	34.6	2.7	3.1	0.6	9.0	26.1	15.4	44.5
Au/Co <sub>3</sub> O <sub>4</sub>	5	44.3	1.2	2.9	0.0	37.2	83.9	41.2	93.0
Au/Co <sub>3</sub> O <sub>4</sub>	20	46.6	2.0	8.5	0.0	44.9	79.3	55.4	97.9
Au/Co <sub>3</sub> O <sub>4</sub>	40	50.5	2.5	7.3	0.2	33.4	66.1	43.4	86.0

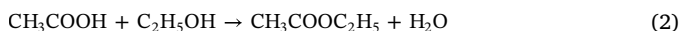
<sup>a</sup> Yield of each product.

**Fig. 1.** In situ ATR-IR spectra during the aqueous phase oxidation of 20 vol% EtOH on Au/Co<sub>3</sub>O<sub>4</sub>, Au/CeO<sub>2</sub>, and Au/NiO catalysts at 120 °C and 3 bar for 2 h. Blueline spectra were taken after 5 min, redline after 2 h. Molecular structures represent bidentate ethoxy species on Au (species 1), multilayered EtOH adsorbed on Au and metal oxide (species 2), on-top ethoxy species on a metal cation of the metal oxide (species 3), and carboxylate species (species 4), respectively.



**Fig. 2.** In situ ATR-IR spectra during the aqueous phase oxidation of EtOH with different EtOH concentrations on Au/Co<sub>3</sub>O<sub>4</sub> at 120 °C, and 3 bar for 2 h. Blueline spectra were taken after 5 min, redline after 2 h. Molecular structures represent bidentate ethoxy species on Au (species 1), multilayered EtOH adsorbed on Au and metal oxide (species 2), on-top ethoxy species on a metal cation of the metal oxide (species 3), and carboxylate species (species 4), respectively.

particles were crucial for the catalytic performance. Employing the best performing catalyst, Au/Co<sub>3</sub>O<sub>4</sub>, we also carried out the reaction using different EtOH concentrations. The conversion increased with the EtOH concentration while the selectivity to AcOH decreased. This behavior can be explained by the balance between the concentrations of EtOH and the produced AcOEt. As the concentration of EtOH is high, the undesired subsequent esterification of AcOH occurs (Eq. 2):



The esterification of AcOH with the residual EtOH affords AcOEt. Employing Co<sub>3</sub>O<sub>4</sub> as support suppressed this undesired consecutive reaction and kept the AcOH selectivity high.

To gain deeper insight into the parameters controlling selectivity and activity, we used in situ ATR-IR spectroscopy. Fig. 1 shows IR

spectra recorded during the aqueous phase oxidation of 20 vol% EtOH on the differently supported Au catalysts at 120 °C and 3 bar for 2 h. Since we had to employ a diamond crystal as IRE, which withstands higher pressure and temperature, the mid-IR region between 1400 and 2200 cm<sup>-1</sup> was cut out due to the intense IR absorption by the phonon mode of the diamond leading to poor or almost no sensitivity [23,25]. At the catalytic solid-liquid interface, EtOH underwent dissociative adsorption via scission of the O–H bond to form ethoxy species (CH<sub>3</sub>CH<sub>2</sub>O-) [26], which possess characteristic IR bands of  $\nu(\text{C}-\text{O})$  at around 1000–1150 cm<sup>-1</sup>. The band at ca. 1120 cm<sup>-1</sup> is assigned to monodentate (also called on-top) ethoxy species on a metal cation of the metal oxide (species 3) [27,28]. The other two bands at ca. 1040 and 1080 cm<sup>-1</sup> originate from bidentate ethoxy (CH<sub>3</sub>CH<sub>2</sub>O-) species adsorbed on Au (designated as species 1) and multilayered EtOH



molecularly-adsorbed on Au and metal oxides (species 2), respectively [27]. The dominant species on the surface depended on the support material; bidentate ethoxy species on Au/Co<sub>3</sub>O<sub>4</sub> and Au/CeO<sub>2</sub>, and multilayered EtOH and on-top ethoxy species on Au/NiO. The selectivity to AcOH was low for Au/NiO, probably due to the preferential dissociative adsorption of EtOH on the NiO support, which contributed to the subsequent esterification of AcOH and/or acetate species to afford AcOEt and Acetal. Two bands at 1300–1340 cm<sup>-1</sup> originate from  $\nu(\text{O-C-O})$  of carboxylate species (species 4) [29,30] typically assigned to surface acetate species on support materials [26]. These bands only decreased slightly on Au/NiO and allowed to consider whether the slow desorption increases the chance for AcOH and/or acetate species to undergo esterification leading to the low selectivity to AcOH. In general, the esterification of aldehydes proceeds more rapidly than that of acids do [31,32]. We cannot exclude the contribution of the esterification route via AcH. However, our data suggest a major contribution of acetate species undergoing unfavorable esterification to produce AcOEt. The best performing catalyst, Au/Co<sub>3</sub>O<sub>4</sub>, showed a negative band at the beginning. Only a short period of 5 min after taking the background was enough for the removal of acetate species as AcOH and also for the reaction of ethoxy species. After 15 min, bidentate ethoxy species and multilayered EtOH started re-accumulating on the surface due to the high conversion of EtOH. On the other hand, carboxylate species took more than 60 min for re-accumulation on the surface. This behavior of surface intermediates accounts for the exceptionally high conversion and selectivity to AcOH on Au/Co<sub>3</sub>O<sub>4</sub>. IR bands at around 2950 cm<sup>-1</sup> are assigned to asymmetric ( $\nu_{\text{as}}$ ) and symmetric ( $\nu_{\text{s}}$ ) stretching vibrations of C–H bonds. Since these bands comprise a variety of surface intermediate species such as ethoxy, acetate, and decomposed hydrocarbonaceous species, they do not provide much information to explain the reaction mechanisms.

To gain a deeper understanding of the effects caused by the EtOH concentration and thus induced selectivity changes, we also performed ATR-IR experiments with the most active catalyst, Au/Co<sub>3</sub>O<sub>4</sub>. As seen in Table 2, the selectivity to AcOH decreased to a certain extent when the EtOH concentration was increased, while the conversion increased. This trend can be well explained by reaction 2, i.e., the esterification of produced AcOH with EtOH. The corresponding ATR-IR spectra are displayed in Fig. 2. With 5 vol% EtOH, on-top ethoxy species prevailed on the surface, whereas bidentate ethoxy species on Au nanoparticles were minor species. This can be the reason why the conversion is low with 5 vol% EtOH. As the concentration increased to 20 vol%, bidentate ethoxy species and multilayered EtOH were prevalent on the surface. Further increase in the concentration to 40 vol% induced the re-emergence of on-top ethoxy species. Because the EtOH concentration and conversion were high, the surface of the Au particles was saturated and the ethoxy species spilled over to the support. This spill-over accelerated the formation of AcOH and thus the undesired consecutive esterification, as highlighted by the emergence of carboxylate species and stretching vibrations of C–H bonds. Judging from the above phenomena observed by ATR-IR analyses, the suppression of the formation of ethoxy species on the support material is a key factor to control the selectivity and activity. The preferential formation of ethoxy species on the Au nanoparticles is favorable for the high catalytic performance of the gold-catalyzed aqueous phase oxidation of ethanol to acetic acid.

#### 4. Conclusions

The gold-catalyzed aqueous phase oxidation of EtOH to AcOH was studied by in situ ATR-IR spectroscopy under real-catalysis working conditions at 120 °C and 3 bar to gain insight into the role of the metal oxide support of the gold nanoparticles in this reaction. The catalytic behaviors of three different catalysts consisting of Au nanoparticles deposited on Co<sub>3</sub>O<sub>4</sub>, CeO<sub>2</sub>, NiO supports were examined. The EtOH conversion on the catalysts followed the order Co<sub>3</sub>O<sub>4</sub> > NiO > CeO<sub>2</sub>, while the selectivity to AcOH obeyed the trend:

Co<sub>3</sub>O<sub>4</sub> > CeO<sub>2</sub> > NiO. In situ ATR-IR spectroscopic investigations proved the presence of four different surface species; (1) bidentate ethoxy species on Au, (2) monodentate ethoxy species on the metal cation of the support, (3) adsorbed multi-layered EtOH, and (4) acetate species on the support. The formation of ethoxy species on the NiO support deteriorated the catalytic performance in terms of both activity and selectivity. Studies on the dependence of the catalytic performance on the EtOH concentration showed that the preferential formation of ethoxy species on the support material (Co<sub>3</sub>O<sub>4</sub>) enhances the catalytic activity accompanied by a decrease in the selectivity to AcOH because of the undesired consecutive esterification of AcOH with EtOH producing AcOEt. To achieve both high activity and selectivity, the selective formation of bidentate ethoxy species on Au nanoparticles with molecularly adsorbed EtOH was found to be crucial.

#### Declaration of Competing Interest

The authors declare that they have no known competing financial interests or personal relationships that could have appeared to influence the work reported in this paper.

#### References

- [1] S. Kim, B.E. Dale, Global potential bioethanol production from wasted crops and crop residues, *Biomass Bioenergy* 26 (2004) 361–375.
- [2] C.J. Liu, J.M. Sun, C. Smith, Y. Wang, A study of Zn<sub>2</sub>Zr<sub>2</sub>O<sub>7</sub> mixed oxides for direct conversion of ethanol to isobutene, *Appl. Catal. A-Gen.* 467 (2013) 91–97.
- [3] C.P. Rodrigues, P.C. Zonetti, C.G. Silva, A.B. Gaspar, L.G. Appel, Chemicals from ethanol-the acetone one-pot synthesis, *Appl. Catal. A-Gen.* 458 (2013) 111–118.
- [4] D.L. Carvalho, L.E.P. Borges, L.G. Appel, P.R. de la Piscina, N. Homs, In situ infrared spectroscopic study of the reaction pathway of the direct synthesis of n-butanol from ethanol over MgAl mixed-oxide catalysts, *Catal. Today* 213 (2013) 115–121.
- [5] A.B. Gaspar, A.M.L. Esteves, F.M.T. Mendes, F.G. Barbosa, L.G. Appel, Chemicals from ethanol-the ethyl acetate one-pot synthesis, *Appl. Catal. A-Gen.* 363 (2009) 109–114.
- [6] E.V. Makshina, W. Janssens, B.F. Sels, P.A. Jacobs, Catalytic study of the conversion of ethanol into 1,3-butadiene, *Catal. Today* 198 (2012) 338–344.
- [7] M. Iwamoto, Selective catalytic conversion of bio-ethanol to propene: a review of catalysts and reaction pathways, *Catal. Today* 242 (2015) 243–248.
- [8] S. Letichevsky, P.C. Zonetti, P.P.P. Reis, J. Celnik, C.R.K. Rabello, A.B. Gaspar, L.G. Appel, The role of m-ZrO<sub>2</sub> in the selective oxidation of ethanol to acetic acid employing PdO/m-ZrO<sub>2</sub>, *J. Mol. Catal. A-Chem.* 410 (2015) 177–183.
- [9] T. Takei, J. Suenaga, T. Ishida, M. Haruta, Ethanol oxidation in water catalyzed by gold nanoparticles supported on NiO doped with Cu, *Top. Catal.* 58 (2015) 295–301.
- [10] G.J. ten Brink, I. Arends, R.A. Sheldon, Green, catalytic oxidation of alcohols in water, *Science* 287 (2000) 1636–1639.
- [11] S.M. Tembe, G. Patrick, M.S. Scurrell, Acetic acid production by selective oxidation of ethanol using Au catalysts supported on various metal oxide, *Gold Bull.* 42 (2009) 321–327.
- [12] T. Takei, N. Iguchi, M. Haruta, Synthesis of acetaldehyde, acetic acid, and others by the dehydrogenation and oxidation of ethanol, *Catal. Surv. Jpn.* 15 (2011) 80–88.
- [13] C.H. Christensen, B. Jorgensen, J. Rass-Hansen, K. Egeblad, R. Madsen, S.K. Klitgaard, S.M. Hansen, M.R. Hansen, H.C. Andersen, A. Riisager, Formation of acetic acid by aqueous-phase oxidation of ethanol with air in the presence of a heterogeneous gold catalyst, *Angew. Chem. Int. Ed.* 45 (2006) 4648–4651.
- [14] K. Mori, T. Hara, T. Mizugaki, K. Ebitani, K. Kaneda, Hydroxyapatite-supported palladium nanoclusters: a highly active heterogeneous catalyst for selective oxidation of alcohols by use of molecular oxygen, *J. Am. Chem. Soc.* 126 (2004) 10657–10666.
- [15] M.C. Greca, C. Moraes, A.M. Segadaes, Palladium/alumina catalysts: effect of the processing route on catalytic performance, *Appl. Catal. A-Gen.* 216 (2001) 267–276.
- [16] L.V. Mattos, F.B. Noronha, Partial oxidation of ethanol on supported Pt catalysts, *J. Power Sources* 145 (2005) 10–15.
- [17] C. Gonzalez-Arellano, A. Abad, A. Corma, H. Garcia, M. Iglesias, F. Sanchez, Catalysis by gold(I) and gold(III): a parallelism between homo- and heterogeneous catalysts for copper-free Sonogashira cross-coupling reactions, *Angew. Chem. Int. Ed.* 46 (2007) 1536–1538.
- [18] K.Q. Sun, S.W. Luo, N. Xu, B.Q. Xu, Gold nano-size effect in Au/SiO<sub>2</sub> for selective ethanol oxidation in aqueous solution, *Catal. Lett.* 124 (2008) 238–242.
- [19] B. Jorgensen, S.E. Christensen, M.L.D. Thomsen, C.H. Christensen, Aerobic oxidation of aqueous ethanol using heterogeneous gold catalysts: efficient routes to acetic acid and ethyl acetate, *J. Catal.* 251 (2007) 332–337.
- [20] T.V. Andrushkevich, V.V. Kaichev, Yu.A. Chesalov, A.A. Saraev, Selective oxidation of ethanol over vanadia-based catalysts: the influence of support material and reaction mechanism, *Catal. Today* 279 (2017) 95–106.
- [21] T. Bürgi, A. Baiker, Attenuated total reflection infrared spectroscopy of solid

- catalysts functioning in the presence of liquid-phase reactants, in: B.C. Gates, H. Knozinger (Eds.), *Advances in Catalysis*, vol. 50, 2006, pp. 227–283.
- [22] A. Waheed, X.W. Wang, N. Maeda, S. Naito, A. Baiker, Surface processes occurring during aqueous phase ethanol reforming on Ru/TiO<sub>2</sub> tracked by ATR-IR spectroscopy, *Appl. Catal. A-Gen.* 581 (2019) 111–115.
- [23] P. Thongnopkun, S. Ekgasit, Attenuated total reflection Fourier transform infrared spectra of faceted diamonds, *Anal. Chim. Acta* 576 (2006) 130–135.
- [24] J.M. Andanson, A. Baiker, Exploring catalytic solid/liquid interfaces by in situ attenuated total reflection infrared spectroscopy, *Chem. Soc. Rev.* 39 (2010) 4571–4584.
- [25] L.J. Su, C.Y. Fang, Y.T. Chang, K.M. Chen, Y.C. Yu, J.H. Hsu, H.C. Chang, Creation of high-density ensembles of nitrogen-vacancy centers in nitrogen-rich type Ib nanodiamonds, *Nanotechnology* 24 (31) (2013) 315702.
- [26] X.Y. Liu, B.J. Xu, J. Haubrich, R.J. Madix, C.M. Friend, Surface-Mediated Self-Coupling of Ethanol on Gold, *J. Am. Chem. Soc.* 131 (2009) 5757.
- [27] D.T. Boyle, J.A. Wilke, R.M. Palomino, V.H. Lam, D.A. Schlosser, W.J. Andahazy, C.Z. Stopak, D.J. Stacchiola, J.A. Rodriguez, A.E. Baber, Elucidation of active sites for the reaction of ethanol on TiO<sub>2</sub>/au(111), *J. Phys. Chem. C* 121 (2017) 7794–7802.
- [28] J.H. Jhang, A. Schaefer, V. Zielasek, J.F. Weaver, M. Bäumer, Methanol adsorption and reaction on Samaria thin films on Pt(111), *Materials* 8 (2015) 6228–6256.
- [29] R.D. Haley, M.S. Tikhov, R.M. Lambert, The surface chemistry of acetic acid on Pd {111}, *Catal. Lett.* 76 (2001) 125–130.
- [30] B.A. Sexton, R.J. Madix, A vibrational study of formic acid interaction with clean and oxygen-covered silver (110) surfaces, *Surf. Sci.* 105 (1981) 177–195.
- [31] T. Ishida, Y. Ogihara, H. Ohashi, T. Akita, T. Honma, H. Oji, M. Haruta, Base-free direct oxidation of 1-Octanol to Octanoic acid and its Octyl Ester over supported gold catalysts, *ChemSusChem* 5 (2012) 2243–2248.
- [32] A. Taketoshi, T. Ishida, T. Murayama, T. Honma, M. Haruta, Oxidative esterification of aliphatic aldehydes and alcohols with ethanol over gold nanoparticle catalysts in batch and continuous flow reactors, *Appl. Catal. A-Gen.* 585 (2019) 117169.